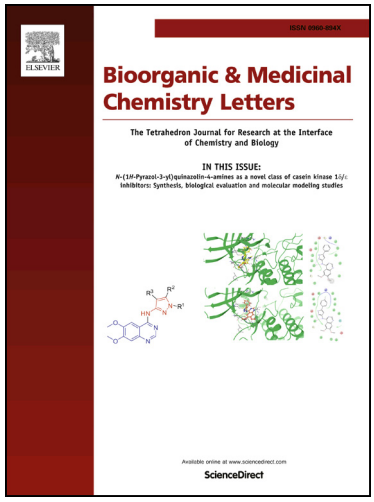

Synthesis and evaluation of 1-phenyl-1*H*-1,2,3-triazole-4-carboxylic acid derivatives as xanthine oxidase inhibitors

Ting-jian Zhang, Qing-xia Wu, Song-ye Li, Lin Wang, Qi Sun, Yi Zhang, Fanhao Meng, Hua Gao

PII: S0960-894X(17)30661-3
DOI: http://dx.doi.org/10.1016/j.bmcl.2017.06.059
Reference: BMCL 25093

To appear in: *Bioorganic & Medicinal Chemistry Letters*

Received Date: 5 April 2017
Revised Date: 17 May 2017
Accepted Date: 22 June 2017

Please cite this article as: Zhang, T-j., Wu, Q-x., Li, S-y., Wang, L., Sun, Q., Zhang, Y., Meng, F-h., Gao, H., Synthesis and evaluation of 1-phenyl-1*H*-1,2,3-triazole-4-carboxylic acid derivatives as xanthine oxidase inhibitors, *Bioorganic & Medicinal Chemistry Letters* (2017), doi: http://dx.doi.org/10.1016/j.bmcl.2017.06.059

Synthesis and evaluation of 1-phenyl-1*H*-1,2,3-triazole-4-carboxylic acid derivatives as xanthine oxidase inhibitors

Ting-jian Zhang [a], Qing-xia Wu [a], Song-ye Li [a], Lin Wang [a], Qi Sun [a], Yi Zhang [a], Fan-hao Meng [a, *], Hua Gao [a, b, *]

[a] *School of Pharmacy, China Medical University, 77 Puhe Road, North New Area, Shenyang 110122, China*

[b] *Division of Pharmacology Laboratory, National Institutes for Food and Drug Control, Beijing 100050, China*

* Corresponding authors.

E-mail addresses: fhmeng@cmu.edu.cn (F-h. Meng), huag55@163.com (H. Gao).

Abstract

This study mainly focused on the modification of the X^2 position in febuxostat analogs. A series of 1-phenyl-1*H*-1,2,3-triazole-4-carboxylic acid derivatives (**1a-s**) with an N atom occupying the X^2 position was designed and synthesized. Evaluation of their inhibitory potency *in vitro* on xanthine oxidase indicated that these compounds exhibited micromolar level potencies, with IC_{50} values ranging from 0.21 μM to 26.13 μM. Among them, compound **1s** (IC_{50} = 0.21 μM) showed the most promising inhibitory effects and was 36-fold more potent than allopurinol, but was still 13-fold less potent than the lead compound Y-700, which meant that a polar atom fused at the X^2 position could be unfavorable for potency. The Lineweaver-Burk plot revealed that compound **1s** acted as a mixed-type xanthine oxidase inhibitor. Analysis of the structure-activity relationships demonstrated that a more lipophilic ether tail (e.g., *meta*-methoxybenzoxy) at the 4′-position could benefit the inhibitory potency. Molecular modeling provided a reasonable explanation for the structure–activity relationships observed in this study.

Keywords: 1,2,3-Triazole; Xanthine oxidase inhibitor; Hyperuricemia.

Xanthine oxidase (XO) is an important enzyme that catalyzes the hydroxylation of both hypoxanthine and xanthine in the last two steps of urate biosynthesis in humans.[1] The over-production of uric acid can lead to hyperuricemia, which is the key cause of gout. Thus, XO is considered the most promising target for treating this pathological condition.[2]

During purine oxidation, XO delivers an electron to the molecular oxygen and generates reactive oxygen species (ROS). An excess of ROS could evoke various pathological states including inflammation, metabolic disorders, atherosclerosis, cancer and chronic obstructive pulmonary disease.[3] Thus, inhibiting XO could reduce the production of ROS and benefit the treatment of these diseases.[4]

Allopurinol is a prototypical XO inhibitor and has been widely used in the treatment of hyperuricemia and gout for several decades. However, in some cases, it has been reported that allopurinol and its analogs, which possess a purine backbone, can lead to severe life-threatening side effects.[5] Therefore, searching for novel non-purine XO inhibitors with more potent XO inhibitory potency but fewer side effects has always been a hotspot. Y-700 is a classic non-purine XO inhibitor that was first reported by Ishibuchi S. *et al.*[6] Although it has not introduced into the market, the excellent activity of Y-700 has widely attracted researchers. Febuxostat[7] is another non-purine XO inhibitor that bears a thiazole moiety and has an outstanding inhibitory potency as well as acceptable side effects and was approved by the US Food and Drug Administration (FDA) in 2009. Thereafter, febuxostat analogs, which are characterized by a five-member aromatic ring linking a benzonitrile moiety and a carboxyl group, have been reported, such as selenazoles,[8] imidazoles[9] and isoxazoles[10] (**Fig. 1**). Furthermore, other XO inhibitors with different structural classes have also been recently reported, including topiroxostat (approved in Japan in 2013),[11] isocytosines,[3, 12] 2-(indol-5-yl)thiazoles,[13] *N*-(1,3-diaryl-3-oxo-propyl)amides,[14] *N*-acetyl pyrazolines,[15] hydroxylated chalcones,[16] 9-deazaguanines,[17] flavonoids,[18] fraxamoside,[19] pyrano[3,2-d]pyrimidine,[20] 2-arylbenzo[b]furan[21] and benzaldehydes.[22]

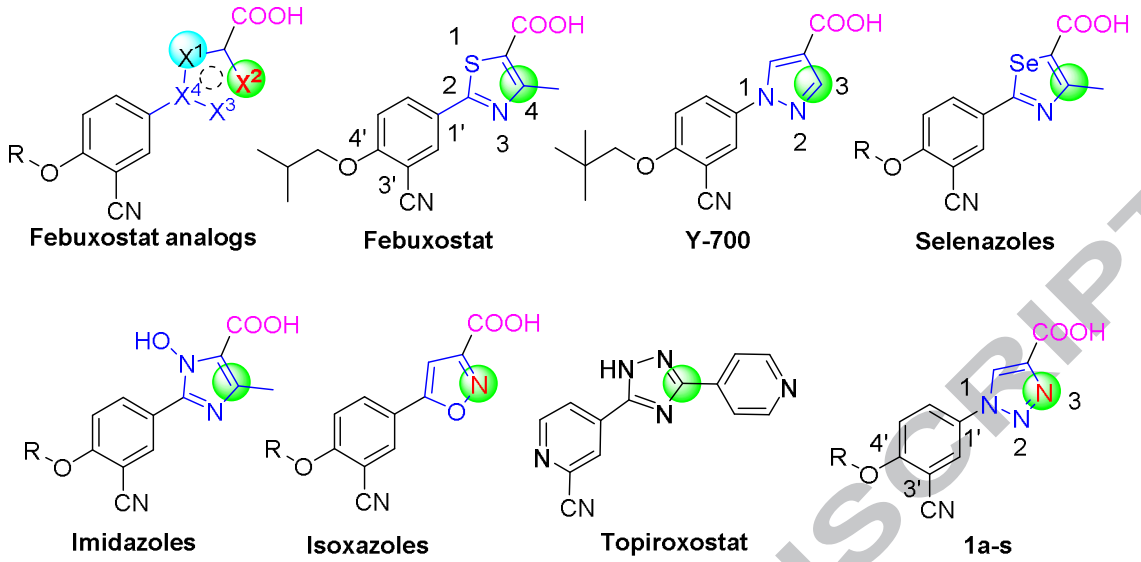

Fig. 1. The chemical structures of some XO inhibitors and designed compounds **1a-s**.

In our previous report, we drew attention to febuxostat analogs of imidazoles[9] and changes in their inhibitory effects due to isosteric replacement at the X^1 position. In this study, we mainly focused on modifications and structure activity relationships (SARs) at the X^2 position. According to the co-crystal structure of XO in complex with Y-700,[23] X^2 is the closest point on the ligand from the molybdenum-pterin, which is the catalytic center of XO. Between them, W498 was observed as a water bridge linked by the H-bonds to the molybdenum-pterin hydroxyl and the Glu1261 carboxyl group.[23] These interactions inspired us and suggest that a polar N atom fixed at the X^2 position may promote some interactions with molybdenum-pterin (e.g., link the molybdenum-pterin by a water bridge) and contribute to the inhibitory potency. Therefore, we designed and synthesized a series of XO inhibitors (**1a-s**) based on 1,2,3-triazole and investigated the effects of a fixed nitrogen atom at the X^2 position in the lead compound Y-700.

The synthesis strategy of target compounds **1** was performed as outlined in **Scheme 1**. Commercially available 2-hydroxybenzonitrile was nitrated in a conc. HNO_3/AcOH system to provide 2-hydroxy-5-nitrobenzonitrile (**2**). The reaction was triggered at 50°C by the addition of a small amount of HNO_3 and maintained by the continuous addition of the remaining HNO_3. During the nitration process, it was essential to carefully control the HNO_3 dropping rate such that the reactive temperature was no higher than 70°C to prevent the

generation of oxidative by-products. In this reaction, a nitro group could also be introduced at the 3-position and generate the by-product 2-hydroxy-3-nitrobenzonitrile. This by-product was difficult to separate out due to its similar polarity, so we employed the mixture directly. A continuous three-step procedure of alkylation with the corresponding alkyl bromide or alkyl chloride followed by reduction using iron powder and isolation with column chromatography effortlessly provided pure 2-alkoxy-5-aminobenzonitriles (**4**). The diazotization of **4** was performed by treatment with sodium azide, which yielded the key intermediate 2-alkoxy-5-azidobenzonitriles (**5**). Cyclization of **5** with ethyl propiolate in the presence of copper sulfate and vitamin C via the Husigen reaction under microwave conditions produced ethyl 1-(4-alkoxy-3-cyanophenyl)-1*H*-1,2,3-triazole-4-carboxylates (**6**), which were hydrolyzed with sodium hydroxide and then acidified to give **1**. The structures of the synthesized compounds were elucidated by ^{1}H NMR, ^{13}C NMR and MS. All the spectral data were in accordance with the assumed structures.

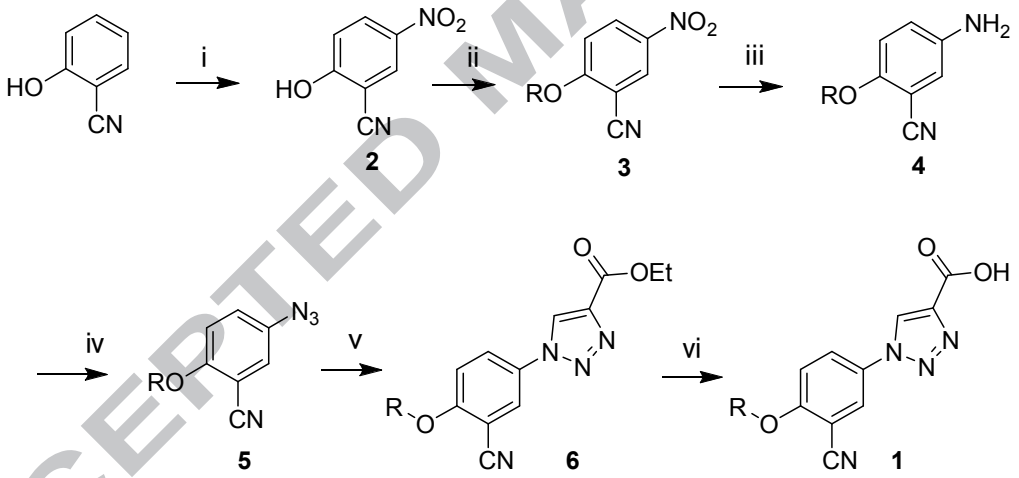

Scheme 1. Reagents and conditions: (i) HNO_3 and AcOH at 50°C for 4 h; (ii) RCl or RBr, K_2CO_3, KI, and DMF at 60°C overnight; (iii) 1) Fe, NH_4Cl, EtOH and H_2O reflux for 3 h followed by 2) isolation by column chromatography (ethyl acetate:petroleum ether = 1:5 to 1:1); (iv) 1) $NaNO_2$, AcOH, and H_2O at -10°C for 30 min followed by 2) NaN_3 at 0°C for 3 h; (v) Ethyl propiolate, $CuSO_4$, and vitamin C at 50°C under microwave conditions for 8 min; and (vi) NaOH, MeOH, and H_2O at 50°C for 1.5 h, followed by the addition of 1 M HCl.

Bovine XO *in vitro* inhibitory potencies by target compounds **1a**–**s** were determined by

spectrophotometrically measuring uric acid levels at 294 nm.[11, 24] Allopurinol and Y-700 were included as reference compounds. The results are shown in **Table 1**.

Table 1. *In vitro* XO inhibitory potency of compounds **1a-s**.

Compound	R group	IC_{50} (μM)
1a	n-propyl	＞30
1b	isopropyl	6.24
1c	n-butyl	5.03
1d	isobutyl	3.27
1e	sec-butyl	3.96
1f	n-pentyl	2.85
1g	isopentyl	1.62
1h	cyclopentyl	1.08
1i	methoxyethyl	26.13
1j	n-hexyl	1.50
1k	n-heptyl	1.47
1l	n-octyl	0.63
1m	benzyl	2.40
1n	*para*-chlorobenzyl	0.94
10	*para*-cyanobenzyl	0.85
1p	*para*-methoxybenzyl	0.72
1q	*ortho*-methoxybenzyl	0.76
1r	*meta*-cyanobenzyl	3.35
1s	*meta*-methoxybenzyl	0.21

Allopurinol	/	7.56
Y-700	/	0.016

According to the literature, an ether side chain containing 3-5 carbons at the 4′-position of febuxostat analogs has been proven to be welcome. Therefore, we initially synthesized a set of compounds bearing an ether chain with 3-5 carbons (**1a-g**) to examine the influence of the various R groups on XO inhibitory potency. Despite having potencies below Y-700 (IC_{50} = 0.016 μM), most of these compounds (except **1a**, IC_{50} >30 μM) showed higher activities compared to allopurinol (IC_{50} = 7.56 μM), which encouraged us to carefully investigate the SAR to identify more effective compounds with potencies comparable to Y-700. Among these compounds, **1g** (IC_{50} = 1.62 μM), which bears an iso-pentyl R group, displayed a higher inhibitory effect. Moreover, a cycloalkyl derivative was involved in the series, and transitioning from the iso-pentyl to cyclopentyl group (**1h,** IC_{50} = 1.08 μM) resulted in a 1.5-fold increase in potency.

Surprisingly, a slight tendency was observed in the **1a-g** subseries that XO inhibitory potency may be gradually improved with increasing R group size. To verify this tendency, a few larger carbon chain derivatives were synthesized, including R = n-hexyl (**1j**, IC_{50} = 1.50 μM), R = n-heptyl (**1k**, IC_{50} = 1.47 μM) and R = n-octyl (**1l**, IC_{50} = 0.63 μM). The results confirmed the existence of this tendency when the R group was prolonged to an n-octyl group. This tendency was distinguished from the Y-700 analogs.[6]

A long carbon chain may lead to the following two effects: (1) increase the bulk and (2) enhance the lipophilicity of the molecule. Due to the flexibility of the R groups and the fact that the febuxostat analog R groups are usually located on the outer region of the XO functional site,[7, 23] which shows less bulk, the lipophilicity may be the primary factor affecting the potency. Therefore, we calculated the log P values of some of the target compounds with the linear R tails (**Fig. 2**) using the *Ligand Properties Tools* in the MOE (Molecular Operating Environment, version 2015.1001) software, and found a negative correlation between the log P and the IC_{50} when the R groups were elongated from n-butyl to n-octyl. Hence, it can be observed that a lipophilic ether tail could benefit the inhibitory

activity of this series; in contrast, a less lipophilic tail may weaken the activity (**1c** versus **1i**).

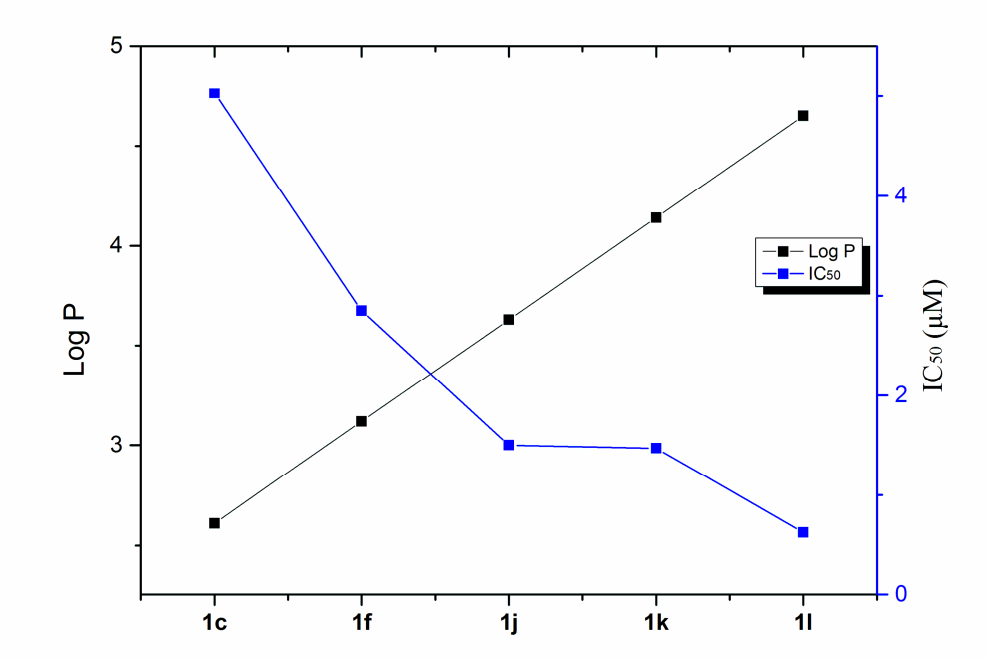

Fig. 2. The log P and IC_{50} values for compounds **1c**, **1f**, **1j**, **1k** and **1l**.

However, a long carbon chain empirically appears to cause some pharmacokinetic issues.[25] Therefore, we alternately attempted to adopt some benzyl groups to play the role of lipophilic tails. Installation of a benzyl as the R group led to **1m** (IC_{50} = 2.40 μM), which exhibited moderate potency. Introduction of some *para*-substituents, such as *para*-chloro (**1n,** IC_{50} = 0.94 μM), *para*-cyano (**1o,** IC_{50} = 0.85 μM) and *para*-methoxy (**1p,** IC_{50} = 0.72 μM), led to 1-3-fold increase in potency. Among these compounds, **1p** showed comparable effects to **1l**. To investigate the influence of the substituent positions, *ortho*- (**1q**, IC_{50} = 0.76 μM) and *meta*- (**1s,** IC_{50} = 0.21 μM) derivatives of **1p** were synthesized. The *meta*-methoxy (**1s**) position was more promising than either the *para*-methoxy (**1p**) or *ortho*-methoxy (**1q**) positions, as the latter two showed almost equal activities. Specifically, **1s** presented an outstanding effect, which was 11-fold enhanced compared to **1m** (R = benzyl) and 3-fold higher than **1l** (R = n-octyl). However, shifting the *para*-cyano (**1o**) to the *meta*-position (**1t**) resulted in a 3.9-fold decrease in potency.

In summary, the most potent compound, **1s**, bears a *meta*-methoxybenzoxy substituent at the 4′-position and displayed an IC_{50} value of 0.21 μM, which was 36-fold more potent than allopurinol, but still 13-fold less potent than Y-700. A steady-state kinetic analysis was

performed to explore the inhibition behaviors of **1s** using the method reported by Matsumoto *et al.*[11] The Lineweaver-Burk plot analysis revealed that **1s** acts as a mixed-type XO inhibitor (**Fig. 3**), and had similar actions to febuxostat[7] and Y-700.[23] This inhibition type could be explained by the potent inhibition of both the oxidized and reduced forms of XO.[26]

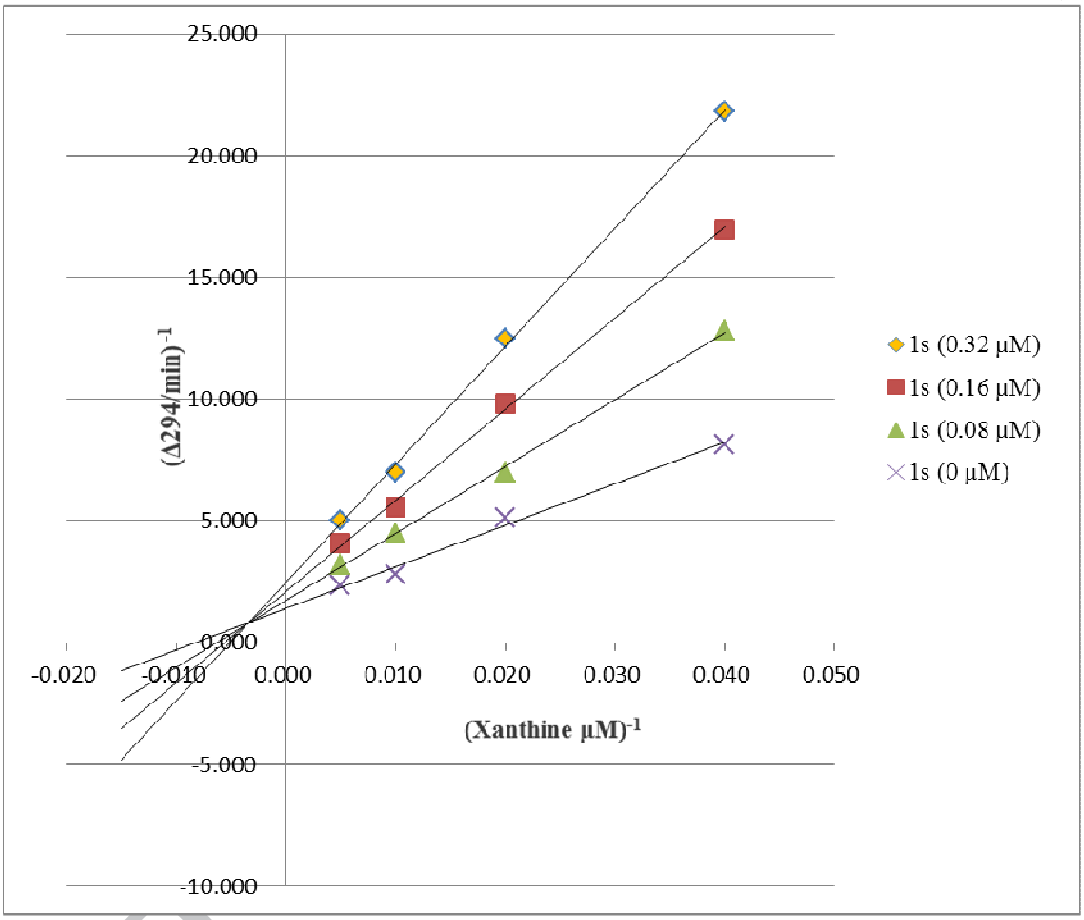

Fig. 3. Lineweaver-Burk plot analysis of xanthine oxidase inhibition by compound **1s**.

Compared with febuxostat,[7] topiroxostat[11] and especially Y-700 (IC_{50} = 0.016 μM), the potency of the 1,2,3-triazoles were obviously lower. This result could be attributed to the replacement of the X^2 carbon atom with the nitrogen atom. The N-3 atom would locally enhance the hydrophilicity and polarity around the X^2 position, which may be the direct cause for the decrease in potency. Similar effects were observed for the isoxazole series.[10] Thus, it can be concluded that a polar atom fused at the X^2 position would be unfavorable for enhancing the potency; inversely, a lipophilic fragment fixed around the X^2 position would benefit the potency. This implies a positive role for the 4-methyl groups in both imidazoles[9] and febuxostat for XO inhibition.

To rationalize the observed SARs, docking simulations of **1s** in the XO binding pocket were performed. The crystal structure of the bovine milk XO/Y-700 complex (PDB code 1VDV) was used as the protein template.[23] A molecular modeling study was undertaken with Autodock 4.[27] An 80 × 80 × 80 Å grid box with a grid spacing of 0.375 Å was generated to define the binding pocket. The Lamarckian genetic algorithm was used as the search parameters. The **1s** carboxyl group was calculated in its dissociated form. The docking model (**Fig. 4**) showed that the **1s** scaffold overlapped with the original ligand very closely. A set of similar binding features were observed, including the carboxylate group interacting with Arg880 and Thr1010, the five-member ring sandwiched between Phe914 and Phe1009[7, 23] and the phenyl moiety cyano group accepting a hydrogen bond from the Asn768 amino group. Moreover, we found that the *meta*-methoxybenzoxy tail was surrounded by several hydrophobic amino acid residues, including Leu648, Phe649, Val1011 and Phe1013, at the entrance to the active site channel. This strong hydrophobic interaction may help anchor **1s** in the XO active site tightly. However, the desired interaction between N-3 and the molybdenum-pterin was not observed; in contrast, the polar N-3 atom, which was located near the center of the Phe914 and Phe1009 sandwich structure, may not be accommodated as well as the corresponding carbon atoms in either febuxostat or Y-700.[7, 23] This suggests that the polar N-3 atom would not enhance the inhibitory potency of the compound. These interactions may provide a reasonable explanation for the gain or loss of the potency at the molecular level.

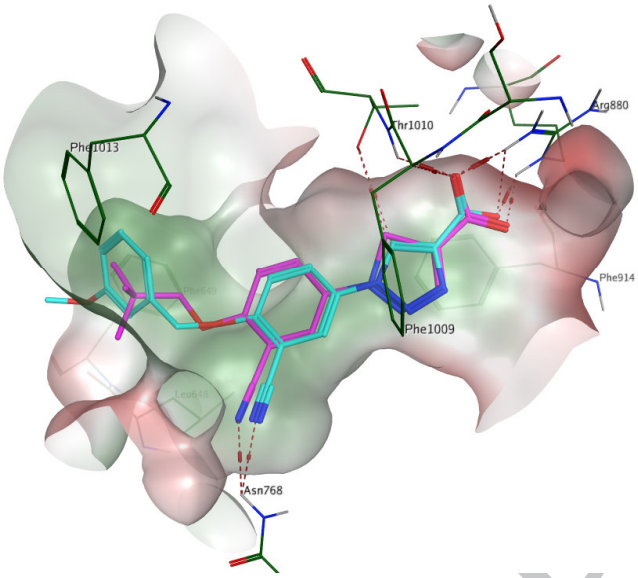

Fig. 4. Docking pose of compound **1s** (cyan) within the protein binding pocket and overlaid with the reference ligand Y-700 (pink).

In summary, a series of 1-phenyl-1*H*-1,2,3-triazole-4-carboxylic acid derivatives (**1a-s**) was designed and synthesized as XO inhibitors. Among them, **1s** was the most promising compound, with IC_{50} value of 0.21 μM and was 36-fold more potent than allopurinol, but 13-fold less potent than Y-700. The Lineweaver-Burk plot revealed that compound **1s** acts as a mixed-type XO inhibitor. The SAR analysis demonstrated that a polar atom fused at the X^2 position would be unfavorable for potency and that a more lipophilic ether tail (e.g., *meta*-methoxybenzoxy) at the 4′-position could benefit the inhibitory potency of these 1,2,3-triazoles. Molecular modeling rationalized the SARs observed in this study. The further detailed investigation on compound **1s** is under progress.

Acknowledgments

This work was supported by the Chinese National Science Foundation (Grant Nos. 81274182 and 81573687) and the project of the Liaoning distinguished professor.

References

1. Gliozzi M, Malara N, Muscoli S, et al. The treatment of hyperuricemia. *Int J Cardiol.* 2016;213:23.

2. (a) Edward R, Michael D. Treatment of hyperuricaemia and gout. *Clin Med.* 2013;13:400; (b) Lü J-M, Yao Q, Chen C. 3,4-Dihydroxy-5-nitrobenzaldehyde (DHNB) is a potent inhibitor of xanthine oxidase: A potential therapeutic agent for treatment of hyperuricemia and gout. *Biochem Pharmacol.* 2013;86:1328.

3. Evenäs J, Edfeldt F, Lepistö M, et al. HTS followed by NMR based counterscreening. Discovery and optimization of pyrimidones as reversible and competitive inhibitors of xanthine oxidase. *Bioorg Med Chem Lett.* 2014;24:1315.

4. (a) Smelcerovic Z, Veljkovic A, Kocic G, et al. Xanthine oxidase inhibitory properties and anti-inflammatory activity of 2-amino-5-alkylidene-thiazol-4-ones. *Chem-Biol Interact.* 2015;229:73; (b) Singh H, Sharma S, Ojha R, et al. Synthesis and evaluation of naphthoflavones as a new class of non purine xanthine oxidase inhibitors. *Bioorg Med Chem Lett.* 2014;24:4192.

5. Pacher P. Therapeutic Effects of Xanthine Oxidase Inhibitors: Renaissance Half a Century after the Discovery of Allopurinol. *Pharmacol Rev.* 2006;58:87.

6. Ishibuchi S, Morimoto H, Oe T, et al. Synthesis and structure–activity relationships of 1-Phenylpyrazoles as xanthine oxidase inhibitors. *Bioorg Med Chem Lett.* 2001;11:879.

7. Okamoto K, Eger BT, Nishino T, et al. An Extremely Potent Inhibitor of Xanthine Oxidoreductase: crystal structure of the enzyme-inhibitor complex and mechanism of inhibition. *J Biol Chem.* 2002;278:1848.

8. Guan Q, Cheng Z, Ma X, et al. Synthesis and bioevaluation of 2-phenyl-4-methyl-1,3-selenazole-5-carboxylic acids as potent xanthine oxidase inhibitors. *Eur J Med Chem.* 2014;85:508.

9. Chen S, Zhang T, Wang J, et al. Synthesis and evaluation of 1-hydroxy/methoxy-4-methyl-2-phenyl-1H-imidazole-5-carboxylic acid derivatives as non-purine xanthine oxidase inhibitors. *Eur J Med Chem.* 2015;103:343.

10. Wang S, Yan J, Wang J, et al. Synthesis of some 5-phenylisoxazole-3-carboxylic acid derivatives as potent xanthine oxidase inhibitors. *Eur J Med Chem.* 2010;45:2663.

11. Matsumoto K, Okamoto K, Ashizawa N, et al. FYX-051: A Novel and Potent Hybrid-Type Inhibitor of Xanthine Oxidoreductase. *J Pharmacol Exp Ther.* 2010;336:95.

12. (a) B-Rao C, Kulkarni-Almeida A, Katkar KV, et al. Identification of novel isocytosine derivatives as xanthine oxidase inhibitors from a set of virtual screening hits. *Bioorg Med Chem.* 2012;20:2930; (b) Khanna S, Burudkar S, Bajaj K, et al. Isocytosine-based inhibitors of xanthine oxidase: Design, synthesis, SAR, PK and in vivo efficacy in rat model of hyperuricemia. *Bioorg Med Chem Lett.* 2012;22:7543; (c) Bajaj K, Burudkar S, Shah P, et al. Lead optimization of isocytosine-derived xanthine oxidase inhibitors. *Bioorg Med Chem Lett.* 2013;23:834.

13. Song JU, Choi SP, Kim TH, et al. Design and synthesis of novel 2-(indol-5-yl)thiazole derivatives as xanthine oxidase inhibitors. *Bioorg Med Chem Lett.* 2015;25:1254.

14. Nepali K, Agarwal A, Sapra S, et al. N-(1,3-Diaryl-3-oxopropyl)amides as a new template for xanthine oxidase inhibitors. *Bioorg Med Chem.* 2011;19:5569.

15. Nepali K, Singh G, Turan A, et al. A rational approach for the design and synthesis of 1-acetyl-3,5-diaryl-4,5-dihydro(1H)pyrazoles as a new class of potential non-purine xanthine oxidase inhibitors. *Bioorg Med Chem.* 2011;19:1950.

16. Hofmann E, Webster J, Do T, et al. Hydroxylated chalcones with dual properties: Xanthine oxidase inhibitors and radical scavengers. *Bioorg Med Chem.* 2016;24:578.

17. Rodrigues MVN, Barbosa AF, da Silva JF, et al. 9-Benzoyl 9-deazaguanines as potent xanthine oxidase inhibitors. *Bioorg Med Chem.* 2016;24:226.

18. Nagao A, Seki M, Kobayashi H. Inhibition of xanthine oxidase by flavonoids. *Biosci Biotech Bioch.*

1999;63:1787.

19. Vitale RM, Antenucci L, Gavagnin M, et al. Structure-activity relationships of fraxamoside as an unusual xanthine oxidase inhibitor. *J Enzyme Inhib Med Chem.* 2017;32:345.

20. Kaur M, Kaur A, Mankotia S, et al. Synthesis, screening and docking of fused pyrano[3,2-d]pyrimidine derivatives as xanthine oxidase inhibitor. *Eur J Med Chem.* 2017;131:14.

21. Tang HJ, Zhang XW, Yang L, et al. Synthesis and evaluation of xanthine oxidase inhibitory and antioxidant activities of 2-arylbenzo[b]furan derivatives based on salvianolic acid C. *Eur J Med Chem.* 2016;124:637.

22. Zhang T-j, Li S-y, Yuan W-y, et al. Discovery and biological evaluation of some (1H-1,2,3-triazol-4-yl)methoxybenzaldehyde derivatives containing an anthraquinone moiety as potent xanthine oxidase inhibitors. *Bioorg Med Chem Lett.* 2017;27:729.

23. Fukunari A, Okamoto K, Nishino T, et al. Y-700 [1-[3-Cyano-4-(2,2-dimethylpropoxy)phenyl]-1H-pyrazole-4-carboxylic acid]: a potent xanthine oxidoreductase inhibitor with hepatic excretion. *J Pharmacol Exp Ther.* 2004;311:519.

24. Kong LD, Zhang Y, Pan X, et al. Inhibition of xanthine oxidase by liquiritigenin and isoliquiritigenin isolated from Sinofranchetia chinensis, Cell. Mol. Life Sci. 57 (2000) 500-505. *Cell Mol Life Sci.* 2000;57:500.

25. (a) Jann MW, Ereshefsky L, Saklad SR. Clinical pharmacokinetics of the depot antipsychotics. *Clin Pharmacokinet.* 1985;10:315; (b) Spanarello S, La Ferla T. The pharmacokinetics of long-acting antipsychotic medications. *Curr Clin Pharmacol.* 2014;9:310.

26. Okamoto K, Nishino T. Mechanism of inhibition of xanthine oxidase with a new tight binding inhibitor. *J Biol Chem.* 1995;270:7816.

27. Morris GM, Huey R, Lindstrom W, et al. AutoDock4 and AutoDockTools4: Automated docking with selective receptor flexibility. *J Comput Chem.* 2009;30:2785.

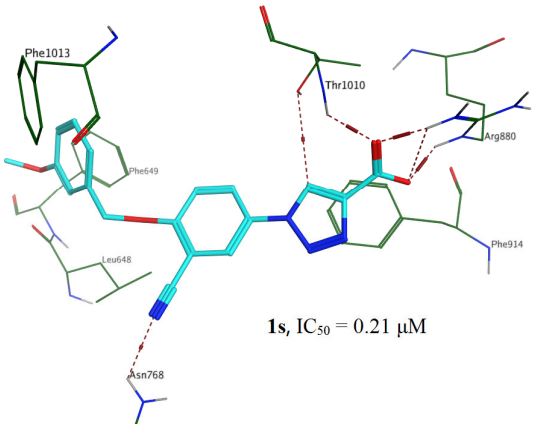

1s, IC_{50} = 0.21 μM